Factors affecting spatial resolution

Gijs J.O. Vermeer, 3DSymSam - Geophysical Advice

Summary

Beylkin's formula for the spatial resolution of surface seismic data is applied to a constant velocity medium. This leads to the same simple resolution formulas for zero-offset data that can be derived in a more heuristic way, and which are in common use in the industry. The results are extended to common-offset data.

Spatial resolution is also analysed by measuring or comparing the widths of the spatial wavelets that are the result of migrating the wavefield of a single diffractor. In this way, a better feeling for the influence of geometry, aperture, sampling and fold can be developed.

A distinction is made between potential resolution – the best possible resolution based on Beylkin's formula, limited by geometry and frequency content of the source –and achievable resolution which is also limited by sampling and noise.

Introduction

The theory of spatial resolution has been dealt with in great detail by various authors on prestack migration and inversion (e.g. Beylkin, 1985, Beylkin et al., 1985, Cohen et al., 1986, Bleistein, 1987), and on diffraction tomography (e.g. Wu and Toksöz, 1987). Despite all this work, the practical consequences of the theory are still open to much debate.

This paper starts with a summary of the main points on spatial resolution as made in Beylkin et al. (1985), and applies this theory to a constant velocity medium. This leads naturally to the same resolution formulas (for 2D data) as given in Ebrom et al. (1995) with an extension to offset data. In the next part I illustrate various aspects of spatial resolution (aperture, offset) using the same simple earth model as von Seggern (1994). Finally, I discuss why sampling is important, even though the sampling interval does not appear in the resolution formulas, and I discuss the influence of fold.

Preliminaries

The theory of resolution leads to a *potential* resolution, i.e., the best possible resolution for a given source wavelet, velocity model, shot/receiver configuration and some position of the output point. The potential resolution does not depend on sampling, because proper sampling of the wavefield is assumed. Next to potential resolution, this paper also uses *achievable* resolution, which is defined as the best possible resolution that can be achieved in less ideal circumstances, such as undersampling and various types of noise. These noises affect the resolvability of two events, hence this achievable resolution is not as good as the potential resolution.

Spatial resolution – the link with migration/inversion

In the literature true-amplitude prestack migration formulas have been derived for *single-fold* 3-D datasets with two spatial coordinates ξ_1 and ξ_2, and traveltime t or frequency f as the third coordinate. ξ_1 and ξ_2 describe the shot/receiver configuration, e.g. $x_\mathbf{s} = (X, Y, 0)$ and $x_\mathbf{r} = (\xi_1, \xi_2, 0)$ describe a 3-D common shot gather, and $x_\mathbf{s} = (\xi_1, Y, 0)$ and $x_\mathbf{r} = (X, \xi_2, 0)$ describe a cross-spread. Note that these data sets are the same datasets introduced as subsets of various 3-D geometries in Vermeer (1994) and which are called minimal data sets by Padhi and Holley (1997).

Beylkin et al. (1985) describe a change of variables from (f, ξ_1, ξ_2) to $(k_\mathrm{x}, k_\mathrm{y}, k_\mathrm{z})$ as follows:

$$\mathbf{k} = f \nabla_x \phi(\mathbf{x}, \boldsymbol{\xi}), \qquad (1)$$

in which $\mathbf{k} = (k_\mathrm{x}, k_\mathrm{y}, k_\mathrm{z})$ is the wavenumber vector in the migration domain, whereas $\phi(\mathbf{x}, \boldsymbol{\xi})$ is the traveltime surface of a diffractor $\mathbf{x} = (x, y, z)$ in the subsurface associated with shot/receiver pairs described by Fout! Bladwijzer niet gedefinieerd.. **Fout! Bladwijzer niet gedefinieerd.**$_x \phi(\mathbf{x}, \boldsymbol{\xi})$ represents the derivative of $\phi(\mathbf{x}, \boldsymbol{\xi})$ with respect to the output point $\mathbf{x}$.

Eq. 1 maps the 5D traveltime surface $\phi(\mathbf{x}, \boldsymbol{\xi})$ to 3D wavenumber. This mapping corresponds to the fact that in prestack migration each input trace described by $\boldsymbol{\xi}$ is used in the reconstruction of a volume of output points (x, y, z). Eq. 1 determines the region of coverage D_X in the spatial wavenumber domain (the 3D spatial bandwidth). Beylkin et al. (1985) state: "*the description of D_X is, in fact, the estimate of spatial resolution.*" The larger the region of coverage in $\mathbf{k}$, the better the *potential* resolution.

Spatial resolution formulas for constant velocity

It is 'illuminating' to investigate D_X for a medium with constant velocity v and a zero-offset geometry. The general formula for $\phi(\mathbf{x}, \boldsymbol{\xi})$ expressed in shot coordinate $\mathbf{x}_\mathrm{S}$ and receiver coordinate $\mathbf{x}_\mathrm{r}$ is:

$$\phi(\mathbf{x}, \xi) = \tau(\mathbf{x}, \mathbf{x}_s) + \tau(\mathbf{x}, \mathbf{x}_r), \qquad (2)$$

where $\tau(\mathbf{x}, \mathbf{y})$ is the traveltime from surface position $\mathbf{y}$ to subsurface position $\mathbf{x}$. For a point $\mathbf{x}_\mathrm{S} = \mathbf{x}_\mathrm{r} = (\xi_1, \xi_2, 0)$, substitution of Eq. 2 into Eq. 1 leads to:

$$\mathbf{k} = 2 \left(\frac{x - \xi_1}{d}, \frac{y - \xi_2}{d}, \frac{z}{d} \right) f / v, \qquad (3)$$

where d is the distance from the coinciding shot and receiver to the subsurface point $\mathbf{x}$.

Factors affecting spatial resolution

Note the difference between horizontal and vertical resolution: k_x, k_y reach their maximum for the maximum

value of d in the x-direction, and y-direction, respectively, whereas k_z reaches its maximum for the minimum value of d, i.e. $d = z$, then $k_z = 2f / v$.

Now select a zero-offset section along the x-axis with $\xi_1 = (-\xi_{max}, \xi_{max})$. Then, for an output point in $(0, 0, z)$ we find

$$k_{x,max} = 2 f_{max} \sin \theta / v; \quad \text{and} \quad k_{z,max} = 2 f_{max} / v, \quad (4)$$

where f_{max} is the maximum frequency, and θ is the angle at $(0, 0, z)$ between the normal to the acquisition line and the raypath to the shot/receiver pairs in $\xi_1 = \pm \xi_{max}$. If we define minimum resolvable distance in a particular direction α as $R_\alpha = 1/2 k_{\alpha,max}$, then:

$$R_x = \frac{v}{4 f_{max} \sin \theta}, \quad \text{and} \quad R_z = \frac{v}{4 f_{max}}. \quad (5)$$

In this way we find the same formulas for horizontal and vertical resolution as given in Ebrom et al. (1995).

Using similar reasoning as above, it follows that for a 2D common-offset gather (shot/receiver azimuth parallel to the x-axis) the minimum horizontally resolvable distance becomes:

$$R_x = \frac{v}{2 f_{max} (\sin \theta_s + \sin \theta_r)}, \quad (6)$$

where θ_s, θ_r is the angle of the normal to the acquisition line with the raypath from the shot, receiver to depth point $(0, 0, z)$, respectively, (for the shot/receiver pair with the largest x-coordinate of the midpoint). Eq. 6 can also be written as

$$R_x = \frac{v}{4 f_{max} \sin \theta \cos i}, \quad (7)$$

where $\theta = (\theta_s + \theta_r) / 2$, i.e., the maximum dip angle illuminated by the shot/receiver pairs, and $i = (\theta_s - \theta_r) / 2$, the angle of incidence of the raypaths for the maximum dip angle. Eq. 7 shows that for a given midpoint range the minimum resolvable distance achievable by offset data is smallest for zero offset ($i = 0$).

Procedure for resolution analysis

Next I illustrate various issues relating to resolution based on a model consisting of a single diffractor in $(0, 0, z)$ in a constant velocity medium. The same model was used in von Seggern (1994). The starting point is a modified version of von Seggern's Eq. 1:

$$f(\mathbf{x}) = c \iint d\xi_1 d\xi_2 h(\mathbf{x}, \xi) p[\phi(\mathbf{x}, \xi) - \phi(0, \xi)] \quad (8)$$

where

$f(\mathbf{x})$ =   image in $\mathbf{x}$

c =   proportionality factor, chosen such that $f(\mathbf{x}) = 1$ for $\mathbf{x} = (0, 0, z)$

p =   constant amplitude wavelet

$h(\mathbf{x}, \xi)$ =   Jacobian of coordinate transformation described in Eq. 1

The integration is over the shots and receivers of the single-fold data set. It should be realised that the validity of Eq. 8 is based on an assumption of continuity of shots and receivers as prescribed by ξ. Sampling of ξ by shots and receivers inevitably leads to some approximation of the integral. The argument of p is the difference in traveltime between a diffractor in the output point and the actual diffractor.

In von Seggern (1991) it was shown that migration of surface data recorded with a Ricker wavelet as a source pulse, produces a Gaussian spatial wavelet in the horizontal directions, but maintains the Ricker wavelet in the vertical direction. Fig. 1 displays the two wavelets along the same distance scale. The Gaussian represents the ideal spatial wavelet.
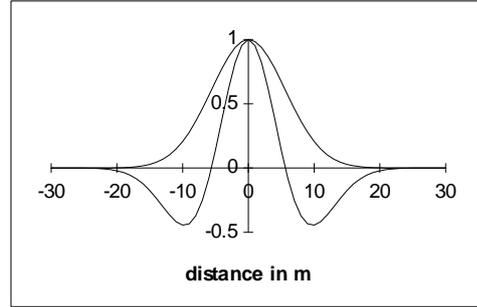

Fig. 1.   The basic spatial wavelets used in this paper. The Ricker wavelet and the Gaussian wavelet have been drawn for an average frequency of 50 Hz and a velocity of 2500 m/s. The Gaussian wavelet is the narrowest achievable bell in prestack migration for the horizontal coordinates.

2D resolution in zero-offset model

For a constant sampling interval of 25 m, and using coinciding shots and receivers along the x-axis, Fig. 2 displays the amplitude of a horizontal trace at the depth of the diffractor (500 m) for various line lengths. The ideal spatial wavelet is also displayed, it virtually coincides with the 6000 m wavelet.

According to Eq. 5 the ideal spatial wavelet, taking dominant frequency rather than maximum frequency, has horizontal resolution of 12.5 m in the example ($v = 2500$ m/s, and $f_d = 50$ Hz). The value of the ideal spatial wavelet at ± 6.25 m can be used as a calibration point by which to measure spatial resolution for various apertures, i.e., the width of the spatial wavelet is measured at that value. Then, for the different line lengths this measured value of $R_{x,meas}$ can be compared with its value computed from Eq. 5. The result is displayed in Fig. 3,

which shows that the width of the spatial wavelet as measured in this way is nearly perfectly representative for the spatial resolution following from $k_{x,max}$.
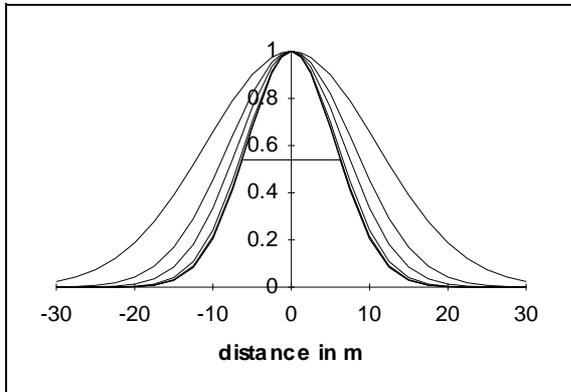

Fig. 2.   Achievable horizontal resolution in a 2D zero-offset geometry for various apertures. From the outside, the wavelets correspond to aperture widths of 600, 1000, 1500, 3000 and 6000 m for a diffractor in (0, 0, 500). The horizontal line in the centre of the figure indicates the level at which widths have been measured for Figs. 3 and 4 (width of ideal wavelet is 12.5 m).
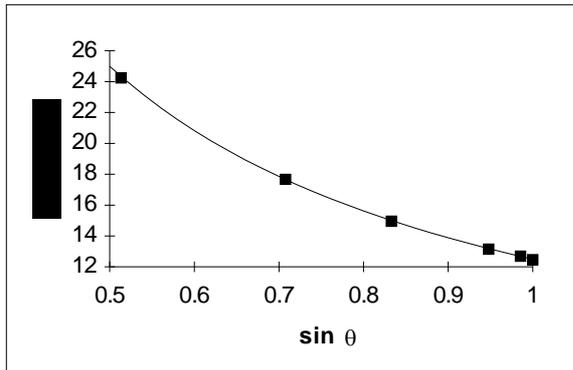

Fig. 3.   Widths of spatial wavelets shown in Fig. 2 plotted against sin θ, θ being the angle between the normal to the acquisition line and the farthest shot/receiver pairs. The drawn curve corresponds to the formula for R_X in Eq. 5, calibrated at θ = 90°.

This result is analogous to the finding in Knapp (1990) that the temporal resolution is proportional to the highest frequency of the data.

2D resolution in offset model

In Figure 4 the results of many different offset experiments have been brought together. Similar as before for Fig. 3, the widths of the spatial wavelets are measured at the same normalised value (black squares), and also computed on basis of Eq. 7 (drawn curves). Each curve represents the results for a single midpoint range. In this case the agreement between predicted value and measured value is not as good as for the zero-offset data in Fig. 3. However, the main trends are caught reasonably well, with increasing discrepancies for increasing line lengths and offsets.

3D spatial resolution

Now select a zero-offset section parallel to the x-axis with ξ_1 = (-ξ_{max}, ξ_{max}) and ξ_2 = Y ≠ 0. For this geometry R_X in (0, 0, z) as computed from Eq. 5 is larger than for a section recorded along the x-axis, because θ is smaller.

As a consequence, if we start with a zero-offset line through the x-axis, and then expand the geometry by adding parallel lines with the same range (-ξ_{max}, ξ_{max}), then k_{max} will not increase, hence the minimum resolvable distance *in the x-direction* cannot decrease. However, the resolution in the y-direction (in fact in *all* other directions) improves.
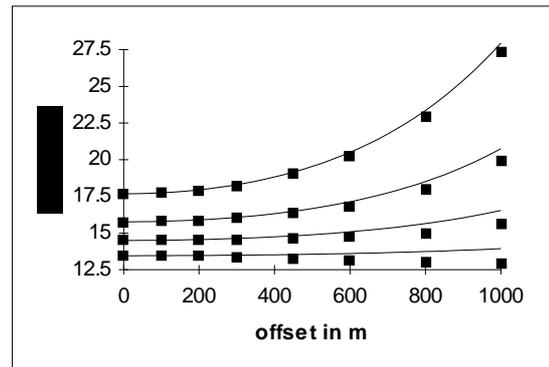

Fig. 4.   Widths of spatial wavelets as a function of offset for line lengths 1000 (top), 1300, 1700 and 2500 m. The drawn curves correspond to Eq. 6, calibrated at zero offset.

This is further investigated in Fig. 5. In this figure the dotted curve represents the ideal spatial wavelet, the next wider curve is the spatial wavelet for a linear spread with length 1000 m along the x-axis, and the heavy line is the spatial wavelet for a 1000 x 1000 m square spread. The widest curve in Fig. 5 corresponds to a linear input spread, again with length 1000 m, but with a crossline distance of 500 m from the x-axis. Fig. 5 demonstrates that for 3D geometries the distribution of k-values in D_X plays a role next to the $k_{x,max}$ of the geometry.
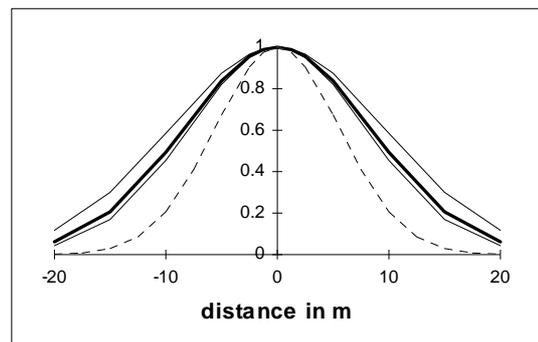

Fig. 5.   Spatial wavelets for constant line length in x, but varying crossline offset. The outer wavelet corresponds to crossline offset 500 m, the thick line to a 1000 x 1000 m areal geometry, and the next wavelet to zero crossline offset. The inner curve is the ideal spatial wavelet.

Sampling and spatial resolution

Factors affecting spatial resolution

The formulas for spatial resolution (Eq. 1 and Eq. 5) do not contain the sampling interval, because these formulas have been derived for a continuous wavefield. When sampling the continuous wavefield, we sample the integrands of the migration formulas such as Eq. 8. If sampling is not rapid enough to keep up with the variations of the integrand, i.e., the integrand is aliased, unreliable results are produced, and resolution will suffer.

Despite the obvious importance of adequate sampling, there is much discussion on the relation between sampling and resolution (Ebrom et al., 1995, Neidell, 1994, Vermeer, 1995, von Seggern, 1994, etc.). Some of the results even seem to indicate that resolution is not significantly impaired by coarse sampling.

Coarse sampling does not influence the resolution of some model experiments, because of the simplicity of the model. This can be illustrated with another simple experiment. In Fig. 6 the spatial wavelets are shown for two 2D geometries with the same line length of 1000 m, but different sampling intervals of 12.5 and 200 m. The wavelets are virtually identical except for the far end. The reason for this seemingly odd result is that the model only consists of the single diffractor. In output points close to the diffractor, the integrand in Eq. 8 varies only slowly as a function of **Fout! Bladwijzer niet gedefinieerd.**. Hence, in this case, the large sampling interval of 200 m is dense enough to follow the variations of the integrand.
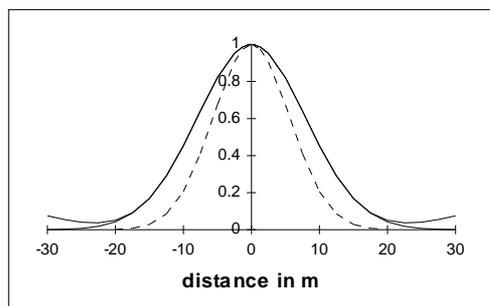

Fig. 6. Independence of spatial wavelet from spatial sampling. The two nearly coinciding outer wavelets correspond to 5 samples @ 200 m and to 80 samples @ 12.5 m. The inner curve is the ideal spatial wavelet.

Fold and spatial resolution

The analysis of spatial resolution as given in Beylkin et al. (1985) deals with single-fold 3D data. If N-fold data are used, ideally, the data can be split into N well-sampled single-fold subsets (Vermeer, 1994). For each subset the potential resolution can be analysed. The resolution of the stack of the N migration results will be some average of the resolutions of the contributing subsets. As the best possible resolution for a given midpoint range can be obtained with a 3D single-fold zero-offset gather, the (potential) resolution of the stack will be less good than the resolution of that zero-offset gather.

In case each contributing subset of an N-fold dataset is undersampled, giving rise to migration noise for each subset, then the stack of the N single-fold migration results would reduce the noise. Now the achievable resolution (in any direction) of the stack of the N migration results should be better than the achievable resolutions of the contributing subsets. Yet, even with very large N, resolution cannot become better than the limit imposed by the maximum frequency in the input data.

Conclusions

In this paper I have linked the description of spatial resolution given in Beylkin et al. (1995) to the more heuristic approach to spatial resolution as given in e.g. Ebrom et al. (1995a). The simple resolution formulas which apply to 2D data provide a lower limit to the minimum resolvable distance that can be achieved with 3D.

The theoretically best possible resolution does not depend on sampling. However, sampling does influence the correctness of the migration process to a large extent, because sampling is a way of approximating the migration integration formulas as derived for continuous shot and receiver variables. Invalid migration results are obtained as soon as the integrand in those formulas varies more rapidly than sampling can follow, i.e., as soon as the data are aliased along the integration paths.

Acknowledgments

References

Beylkin, G., 1985, Imaging of discontinuities in the inverse scattering problem by inversion of a causal generalized Radon transform: J. Math. Phys. **26**, 99-108.

Beylkin, G., Oristaglio, M., and Miller, D., 1985, Spatial resolution of migration algorithms: *in* Berkhout, A.J., Ridder, J., and van der Waals, L.F., Eds., Proceedings of the 14th Internat. Symp. on Acoust. Imag., 155-167.

Cohen, J.K., Hagin, F.G., and Bleistein, N., 1986, Three-dimensional Born inversion with an arbitrary reference: Geophysics, **51**, 1552-1558.

Ebrom, D., Li, X., McDonald, J., and Lu, L., 1995a, Bin spacing in land 3-D seismic surveys and horizontal resolution in timeslices: The Leading Edge, **14**, 37-40.

Knapp, R.W., 1990, Vertical resolution of thick beds, thin beds, and thin-bed cyclothems: Geophysics, **55**, 1183-1190.

Neidell, N.S., 1994, Sampling 3-D seismic surveys: A conjecture favoring coarser but higher-fold sampling: The Leading Edge, **13**, 764-768.

Padhi, T., and Holley, T.K., 1997, Wide azimuths – why not?: The Leading Edge, **16**, 175-177.

von Seggern, D., 1991, Spatial resolution of acoustic imaging with the Born approximation: Geophysics, **56**, 1185-1202.

von Seggern, D., 1994, Depth-imaging resolution of 3-D seismic recording patterns: Geophysics, **59**, 564-576.

Vermeer, G.J.O., 1994, 3-D symmetric sampling: 64th Ann. Internat. Mtg., Soc. Expl. Geophys., Expanded Abstracts, 906-909.

Vermeer, G.J.O., 1995, Is "coarse" the right course?: The Leading Edge, **14**, 989-993, with reply by N. Neidell.

Wu, R-S, and Toksöz, M.N., 1987, Diffraction tomography and multisource holography applied to seismic imaging: Geophysics, **52**, 11-25.